

RESEARCH ARTICLE SUMMARY

ICE SHEETS

Slowdown in Antarctic mass loss from solid Earth and sea-level feedbacks

E. Larour*, H. Seroussi, S. Adhikari, E. Ivins, L. Caron, M. Morlighem, N. Schlegel

INTRODUCTION: Geodetic investigations of crustal motions in the Amundsen Sea sector of West Antarctica and models of ice-sheet evolution in the past 10,000 years have recently highlighted the stabilizing role of solid-Earth uplift on polar ice sheets. One critical aspect, however, that has not been assessed is the impact of short-wavelength uplift generated by the solid-Earth response to unloading over short time scales close to ice-sheet grounding lines (areas where the ice becomes afloat). Here, we present a new global simulation of Antarctic evolution at high spatiotemporal resolution that captures solid-Earth processes stabilizing and destabilizing ice sheets. These include interactions with global eustatic sea-level rise (SLR), self-attraction and loading (SAL) of the oceans, Earth's rotational feedback to SAL, and elastic uplift of the solid Earth.

RATIONALE: In Antarctica, dynamic thinning and retreat of ice streams has been the main driver of mass loss over the past decades, largely controlled by how grounding lines migrate and interact with bedrock pinning points. Studies have shown that the physical representation of grounding-line dynamics (GLD) can only be captured through simulations with a horizontal resolution higher than 1 km. Current models of SLR that incorporate solid-Earth processes with viscoelastic response tend to involve GLD that is resolved at much coarser resolutions (25 to 100 km) and involve time steps on the order of decades. Such resolution bounds are incompatible with capturing the complex bed topography of the ice streams of West Antarctica that are vulnerable to rapid retreat. In addition, a resolution of 25 to 100 km is inherently too coarse to capture short-wavelength elastic uplift generated by fast GLD. Elastic uplift gen-

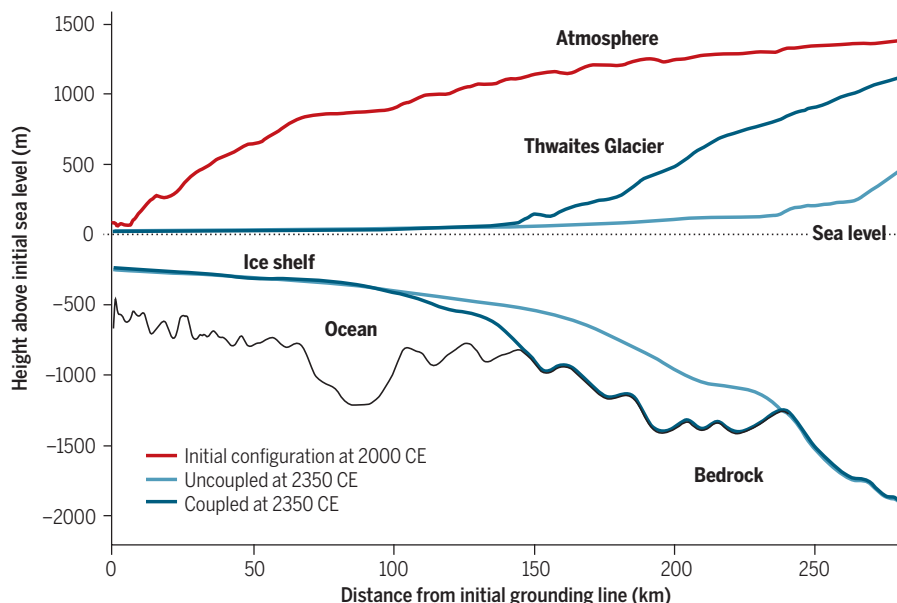
erated by a 2-km grounding-line retreat, modeled as loss of 100-m-thick ice from a disk of 2-km radius, can reach 52 mm near the grounding line (centroid of the equivalent disk). At coarser resolutions (say, 16 km), the same model generates uplift one order of magnitude lower. This implies that uplift generated in simulations at coarse resolutions might underestimate how much uplift is generated during ungrounding

of active areas of Antarctica such as Thwaites Glacier (TG), where highly complex grounding-line geometries and associated retreat are observed over short time scales on the

order of years. Our goal was therefore to carry out a sensitivity study of sea level- and ice flow-related processes that incorporate kilometer-scale resolutions and global processes involving solid-Earth dynamics.

RESULTS: Our sensitivity study spans 500 years and demonstrates how in Antarctica, TG is particularly prone to negative feedback from SAL and elastic uplift. At year 2350, including these feedbacks leads to a ~20-year delay in dynamic mass loss of TG, corresponding to a 26.8% reduction in sea-level contribution, along with a reduction in grounding-line retreat of 38% and elastic uplift rates reaching ~0.25 m/year. At year 2100, though, this negative feedback is considerably lower, with a 1.34% reduction in sea-level contribution only. Not including a kilometer-scale resolution representation of such processes will lead to projections of SLR that will significantly overestimate Antarctic Ice Sheet contribution over several centuries.

CONCLUSION: For 21st-century projections, the effects we have modeled here remain negligible. However, for the period starting 2250 and after, SLR projections that would not account for such dynamic geodetic effects run the risk of consistently overestimating (by 20 to 40%) relative sea-level estimates. Our approach shows that significant stabilization in grounding-line migration occurs when uplift rates start approaching 10 cm/year. This has strong implications for late Quaternary reconstructions of SLR, for example, in which the inclusion of these solid-Earth processes will allow SLR modelers to gain a better grasp of the time scales involved in reaching maximum coastal inundation levels during extended warm periods. ■



Sensitivity study of TG, Antarctica, 350 years into the future. Red, present-day surface of TG; dark blue, TG at 2350 CE without SLR or solid-Earth processes included in the simulation; light blue, configuration for a simulation that includes coupled SLR and solid-Earth processes; dotted black and solid black, present-day sea-level and bedrock position, respectively.

The list of author affiliations is available in the full article online.

*Corresponding author. Email: eric.larour@jpl.nasa.gov

Cite this article as E. Larour et al., *Science* **364**, eaav7908 (2019). DOI: 10.1126/science.aav7908

RESEARCH ARTICLE

ICE SHEETS

Slowdown in Antarctic mass loss from solid Earth and sea-level feedbacks

E. Larour^{1,2*}, H. Seroussi¹, S. Adhikari¹, E. Ivins¹, L. Caron¹, M. Morlighem³, N. Schlegel¹

Geodetic investigations of crustal motions in the Amundsen Sea sector of West Antarctica and models of ice-sheet evolution in the past 10,000 years have recently highlighted the stabilizing role of solid-Earth uplift on polar ice sheets. One critical aspect, however, that has not been assessed is the impact of short-wavelength uplift generated by the solid-Earth response to unloading over short time scales close to ice-sheet grounding lines (areas where the ice becomes afloat). Here, we present a new global simulation of Antarctic evolution at high spatiotemporal resolution that captures all solid Earth processes that affect ice sheets and show a projected negative feedback in grounding line migration of 38% for Thwaites Glacier 350 years in the future, or 26.8% reduction in corresponding sea-level contribution.

Geodetic investigations of crustal uplift in the Amundsen Sea sector (ASS) of West Antarctica (1) and models of grounding-line retreat followed by readvance in the Ross Sea sector during the past 10,000 years (2) have recently highlighted the stabilizing role of solid-Earth uplift on polar ice sheets. The specific processes involved in this negative feedback have previously been extensively investigated, such as self-attraction and loading (SAL) (3), rotational feedback (4), and redistribution of mass in the Earth due to glacial isostatic adjustment (GIA) (5, 6). Some of these processes, SAL and GIA in particular, have been shown to stabilize grounding-line retreat of ice sheets resting on retrograde slope (7–9).

Our focus is on how short-wavelength uplift generated by the unloading of Earth's crust over short time scales in the immediate vicinity of grounding lines further affects the dynamics of ice sheets' grounding-line migration, which has not previously been investigated. Grounding lines in Antarctica are geographically refined features that need to be spatially resolved at resolutions less than 1 km (10) and that migrate over short time scales (weeks to months) (11), which triggers the question of how to avoid underestimating the resulting uplift upon migration. Our global simulation of Antarctic evolution presented here is carried out at the

necessary high temporal resolution (14 days and 365 days for the ice and solid Earth, respectively) and spatial resolution (1 to 50 km) required to capture the processes that stabilize and destabilize ice sheets. These include interactions that involve global eustatic sea-level rise (SLR), SAL, elastic rebound of the solid Earth, and rotational feedback.

In Antarctica, dynamic retreat of ice streams has been the main driver of mass loss (12). These ice streams are largely controlled by how their grounding lines migrate (13) and interact with pinning points (14). Recent research efforts have focused on the complex interactions between intrusion of warm circumpolar water near the grounding line (11), ungrounding of pinning points (14, 15), and reduction in buttressing through loss of friction (16). A key aspect of understanding grounding-line dynamics (GLD) is to understand the relationship between the evolving sea level and the exact position of pinning points. As shown through NASA's Operation IceBridge topographic mapping as well as decades-long efforts to map grounding-line migration, highly resolved pinning points are present in critical areas of the West Antarctic Ice Sheet (WAIS) that can only be captured at kilometer-scale resolutions (17, 18). In parallel, studies have shown that the physical representation of grounding-line migration can only be modeled through meshes that attain 1-km resolution (19). There has been recent interest in developing future projections of SLR that incorporate solid-Earth processes with Maxwellian viscoelastic response (7–9) and SAL (7, 20). However, these tend to involve GLD that is resolved at much coarser resolutions (25 to 100 km) and involve time steps on the order of years or even

decades. Such resolution bounds are incompatible with capturing the complex geometry of WAIS ice streams that are vulnerable to rapid retreat. For example, Pine Island Glacier (PIG) is 20 to 30 km wide at the grounding line, with complex grounding-line geometry that can only be resolved spatially at the 1- to 2-km level (10).

In addition, a resolution of 25 to 100 km is inherently too coarse to capture short-wavelength elastic uplift generated by fast grounding-line retreat and associated mass loss. As shown in Fig. 1, elastic uplift generated by a 2-km grounding-line retreat, modeled as loss of 100-m-thick ice from a disk of 2-km radius, can reach 52 mm near the grounding line (centroid of the equivalent disk). At coarser resolutions (say, 16 km), the same model generates uplift one order of magnitude lower. This implies that uplift generated in simulations such as (7–9) might underestimate how much uplift is generated during ungrounding of active areas of Antarctica such as Thwaites Glacier (TG) or PIG, where highly complex grounding-line geometries and associated retreat are observed over short time scales on the order of years. Some models, such as (21), have attained resolutions down to 6 km; however, in such cases GLD has not been considered interactively but prescribed offline, which precluded extensive negative feedback from manifesting themselves during the simulations. Our goal was to carry out a sensitivity study of sea level- and ice flow-related processes by incorporating kilometer-scale resolutions and global processes that involve solid-Earth dynamics. The ice-flow model robustly captures GLD at high resolution (1 km) and over very short time scales (2 weeks).

To understand the impact of solid-Earth dynamics, we needed to independently assess the role of each process. Our strategy was to incrementally introduce the following processes: (i) eustatic sea level; (ii) SAL of the ocean; (iii) elastic response of the solid Earth; (iv) elastic rotational feedback; and (v) background GIA (BGIA), considered here as an offline component and not an interactive model. Each of these processes includes the previous ones. To evaluate all of these processes, we relied on a control run capturing the traditional approach of ice-sheet models, in which ice-sheet evolution is independent of relative sea level (RSL) and other solid-Earth processes. We define this model as UNC (or uncoupled) (Fig. 2A and Table 1). RSL trends are recovered from UNC and similar types of models (22) by an *a posteriori* transfer of total mass loss to the ocean, leading to a global and uniform increase in sea level.

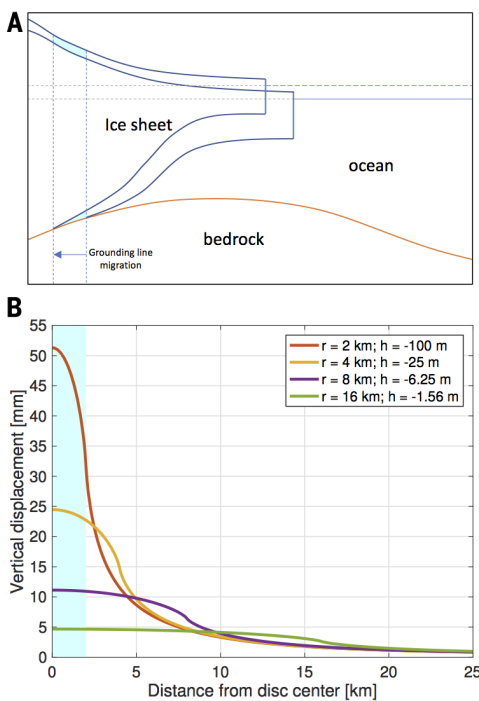
To account for the effects of eustatic sea level on ice dynamics, we relied on a model we term EUS (Fig. 2B and Table 1), where an update to RSL at the ice front is computed, thus modifying the pressure exerted by the ocean on ice-calving fronts as well as ice shelves' hydrostatic equilibrium. The eustatic increase in RSL originates in mass loss from all major glaciated areas of the world (ice sheets and glaciers). Essentially, as captured by the EUS model, an increase in RSL

¹Jet Propulsion Laboratory, California Institute of Technology, Pasadena, CA, USA. ²Joint Institute for Regional Earth System Science and Engineering, University of California, Los Angeles, Los Angeles, CA, USA. ³Department of Earth System Science, University of California, Irvine, Croul Hall, Irvine, CA, USA.

*Corresponding author. Email: eric.larour@jpl.nasa.gov

Fig. 1. GLD, unloading, and spatial resolution effects on solid-Earth deformation.

(A) A sketch of dynamic evolution of an ice sheet/ice shelf system in which ice thinning at the grounding line results in migration and unloading of the underlying bedrock. The equivalent amount of ice (if thinning is neglected) that is removed from the bedrock is shaded in light blue. (B) Vertical displacement from unloading of this ice, modeled as a cylindrical load of ice [radius (r) = 2 km by height (h) = 100 m] that melts away. Effects of spatial resolution are explored by mapping the same volume of ice melt on to coarser disks having r = 16, 8, and 4 km, respectively. A 2-km resolution model can realistically capture the concentrated load and predicts substantial uplift, whereas a coarse-resolution model generates vertical displacement in the near field up to one order of magnitude lower. All of these simulations were performed for the Preliminary reference Earth model (PREM), having a continental crust (surface layer) with Lame parameters μ = 26.624 GPa (1 GPa = 10^9 Pa) and λ = 34.216 GPa.



lifts an ice shelf upward, resulting in grounding-line retreat, which leads to a positive feedback (23). However, as ice mass is lost, the local gravity attraction drops, resulting in reduced hydrostatic pressure at calving fronts. To account for this gravity of the ocean mass, we relied on the model we term SAL (Fig. 2C and Table 1), where the computation of RSL results in a negative feedback (7). The SAL model accounts for a rigid Earth in order to fully isolate its effects from the vertical motions of a compressible and seismologically constrained realistic Earth. To account for the effects of the elastic response of the solid Earth, we relied on a model that we define as ELA (Fig. 2D and Table 1), where we remove the hypothesis of a rigid Earth (1) and introduce elastic uplift of the bedrock in response to the ice mass loss unloading the Earth crust and associated sea-surface height. On marine sectors of the ice sheet, uplift tends to yield decreased grounding-line retreat (8). To account for effects owing to rotational feedback, we relied on the ROT model (Fig. 2E and Table 1), where we add rotational feedback effects attributable to global-scale mass redistribution associated with SAL and elastic deformation. The resulting computation of RSL (3, 24, 25) tends to lower the RSL in the vicinity of mass loss and feature long wavelengths, thus potentially introducing a slight negative feedback in grounding-line migration. Last, for BGIA effects, we did not model GIA interactively but rather relied on a precomputed offline background GIA time series that is superimposed on all other processes (Fig. 2F and Table 1, model run we term NSM for net sum model of all processes referred to above). This BGIA time series comes from a recent Bayesian global study by (26) that used Maxwellian

viscoelasticity and that took into account variations in RSL on a compressible self-gravitating, rotating Earth owing to the response of the solid Earth to past ice and ocean mass changes. This response occurs over longer time scales (century and longer scales) and also tends to reduce grounding-line migration through uplift of the bedrock (1, 2, 7–9). Although rotational feedback occurs both on the BGIA and elastic time scales independently, we investigated and isolated the elastic rotational feedback contribution. We do include the rotational feedback contribution from BGIA in the computational scheme, but only as an *a posteriori* offline process. What is distinct about our subsequent investigation is the role played by the elastic response because this has seemingly been overlooked in all past studies owing to resolution limitations imposed by attempting to deal with Maxwellian viscoelasticity. Our goal was, therefore, to thoroughly quantify the impact of elasticity before attempting more complex interactions with Maxwellian or more advanced transient solid-Earth rheologies.

Model and setup

In order to solve for all the aforementioned processes, we were compelled to solve for both RSL and ice flow at high spatial resolution. For ice sheets, grounding-line migration needs to be captured at the 1-km-resolution level [Marine Ice Sheet Model Intercomparison Project for planview models 3D (MISMIP3d)] (19). This resolution is necessary to capture feedbacks between ice-flow dynamics and the bedrock topography. For RSL, knowledge of bedrock uplift and absolute sea level (ASL) is the prerequisite for application of the hydrostatic equilibrium criterion, which

modulates the pace of grounding-line migration. This implies that SAL, ELA, and ROT models need to be solved at kilometer-scale resolutions near grounding lines or at least need to be investigated for their sensitivity to spatial resolutions (Fig. 1). Our working assumption is that by exploring the impact of kilometer-scale resolution in model representation of grounding-line retreat, the one-order-of-magnitude increase in uplift as isolated in our single cap unloading (Fig. 1) will generate significant negative feedback in the SAL, ELA, and, potentially, ROT models. The Ice Sheet System Model (ISSM) is an ice-flow modeling software (27) that is based on anisotropic unstructured meshes using the finite element method. It is therefore capable of meeting these requirements to capture GLD at 1-km-scale resolution (11), using anisotropic mesh refinement and higher-order thermomechanical representation of ice-flow dynamics (11). Recently, a global sea-level model that can capture SAL effects, elastic vertical uplift, and elastic rotational feedback down to kilometer-scale resolutions was formulated (28) and implemented in ISSM (25, 28). This formulation can model RSL at the grounding line of ice sheets with resolutions compatible with ISSM's higher-resolution grounding-line migration, hence enabling a quantitative assessment of all solid-Earth-related feedbacks. We implemented a full two-way coupling between the ice-flow and RSL formulations, in which the entire Antarctic ice sheet was fully represented in terms of mass transport, stress balance, and grounding-line migration, as well as melting rate forcing under every ice shelf [using a calibrated melt-rate parameterization (11)], and interacted with a full global-scale RSL simulation in which sea-level and bedrock uplift are computed and refined to high resolutions along Antarctica's grounding lines. The scope of the analysis is not to carry out a fully realistic projection of Antarctica but rather to capture the forcing that we currently understand as being responsible for grounding-line retreat. This is why we relied on a state-of-the-art melt-rate parameterization but did not carry a realistic but uncertain climatology projection. For all other glaciated areas of the world where ice thickness changes are required to source the RSL model, we did not run stress-balance and grounding-line migration models but rather implemented a simple mass-transport scheme in which ice thickness changes were locally constrained to match observed Gravity Recovery and Climate Experiment (GRACE) mass trends from 2003 to 2016 (29). This implies that except for Antarctica, all other glaciated areas are contributing a constant amount of melt to the oceans, without feedback on ice-flow dynamics. This assumption is conservative because the contribution of Greenland and other glaciers in the world to RSL is currently understood to significantly increase by the end of the century, but given that our goal is to understand the impact of Antarctica on RSL and vice versa, our control run and experiments needed to experience a modestly realistic RSL increase coming from other glaciated areas while

not resulting in further ice-flow dynamic feedbacks. This also implies that our simulations would capture processes for which the timing might not be fully realistic but compatible with conditions in which elastic feedbacks will manifest, such as during the collapse of TG. We strove to reach conclusions that can be adapted for

other timelines and, in particular, for more realistic projections of Antarctica.

Given that we are interested in the impact on short time scales and not on longer time scales, the six models can all be initialized identically by using an instantaneous ice-flow spin-up referenced to year 1999 (supplementary materials,

materials and methods) followed by a 1-year relaxation, fully uncoupled from any RSL or solid-Earth process. This can only be done because we do not rely on past history of ice deformation required for a viscous formulation. Starting the model at year 2000, physical processes described in Fig. 2 were activated for EUS, SAL, ELA, ROT, and NSM scenarios. The UNC model run was used as a control run. All runs were carried out for 500 years starting from the exact same configuration at model year 2000.

Results

Comparing each model run to the UNC control run, we can demonstrate the critical impact that solid-Earth deformation and SAL effects have on the evolution of Antarctica, both in terms of grounding line retreat as well as resulting contribution to SLR around the world. The global fingerprint of ASL 350 years into the future for the UNC, EUS, ELA, SAL, ROT, and NSM models is shown in Fig. 3 and fig. S18. The dynamic retreat of TG and PIG is clearly visible (as a local collapse in RSL), with associated strong patterns of sea-level fingerprints in the Pacific Ocean. The impact of SAL (Fig. 3A) is substantial, as well as elastic uplift (Fig. 3, A and B). The ROT model exhibits, as expected for a collapsing WAIS (30, 31), strong patterns particularly along the Indian Ocean and North Pacific. Although such effects are expected in terms of global sea-level fingerprint (24, 31), their local expression in terms of grounding-line migration is not well understood. In Fig. 4, we assess the magnitude and scale of such feedbacks on the evolution of the WAIS grounding line. By 2350, the grounding line in the UNC model has propagated on average 240 km upstream of its initial position (Fig. 4, red versus black lines). There is a slight difference

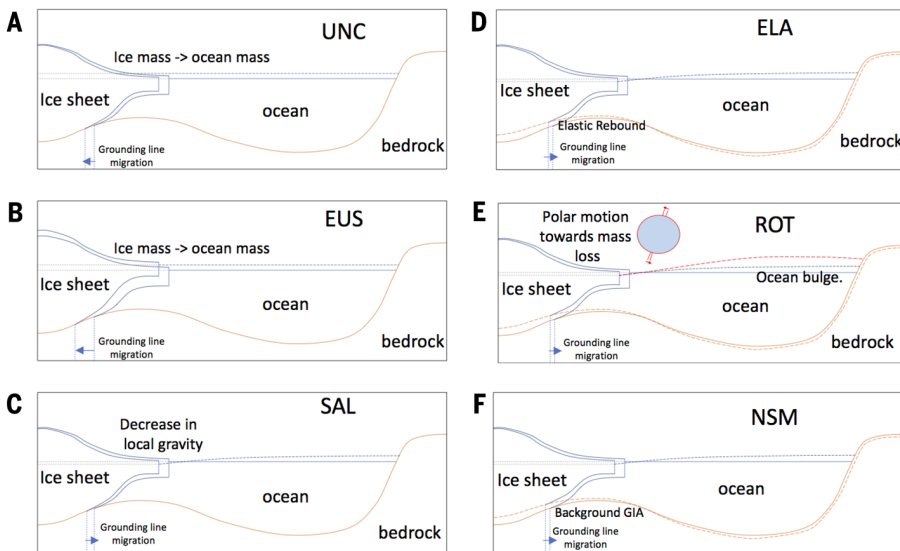


Fig. 2. Processes involved in a dynamically interactive ice sheet/solid-Earth system model.

Models are (A) UNC, (B) EUS, (C) SAL, (D) ELA, (E) ROT, and (F) NSM. A description of the different models and how they incrementally introduce feedbacks into the ice evolution is given in Table 1. For each model, we indicate how grounding-line migration is affected, as well as local and far-field RSL. For the ELA, ROT, and NSM models, we also show how sea-level change affects solid-Earth deformation of the bedrock. Solid and dashed lines represent initial and final configurations, respectively. The direction of GL migration is indicated with arrows. Ice-flow dynamics and forcing from melt rates generated by our ice–ocean interaction parameterization will generate a finite GLD, as indicated in (A), the UNC case.

Table 1. Model labels and definitions. For each model, a label is provided along with a corresponding description of the physical processes represented and levels of feedback between the RSL and ice-sheet model. In addition, modeled relative differences (in percent) in GLD against the UNC control run are provided. This difference is measured along the gray flowline (Fig. 4, bottom) for the year 2350. A positive value indicates a positive feedback (where the grounding line

migrates further upstream than the control run). A negative value indicates the opposite, with the evolutionary fate of the grounding line drifting downstream of the UNC grounding line position. Brackets indicate a range of values. Similarly, relative difference in TG volume above flotation and TG volume change (in percent of sea-level equivalent) is provided against UNC for three epochs: 2100, 2350, and 2500.

Model	Description	GLD feedback (%)	TG volume above flotation feedback (%) 100/350/500 years	TG volume feedback (%) 100/350/500 years
UNC	Ice-sheet evolution independent of RSL (uncoupled). A posteriori transfer of mass loss to the ocean. Spatially uniform increase in RSL. RSL update as ice sheets evolve.	0	0/0/0	0/0/0
EUS	Eustatic transfer of ice mass loss to the ocean. Spatially uniform increase in RSL.	[0 to 1]	-0.2/1.2/0.69	0.09/1.65/0.51
SAL	EUS model + RSL fingerprint accounting for self attraction and loading from ocean on a self-gravitating, rigid Earth.	-10.6	-0.82/-7.8/-2.1	-0.18/-7.17/-0.6
ELA	SAL model + elastic uplift.	-38	-29/-29.5/-16.7	-1.26/-26.8/-9.2
ROT	ELA model + elastic rotational feedback.	-38	-29/-29.5/-16.9	-1.26/-26.8/-9.2
NSM	ROT model + BGIA adjustment.	-38.5	-43.9/-31.7/-18.5	-1.34/-28.4/-9.9

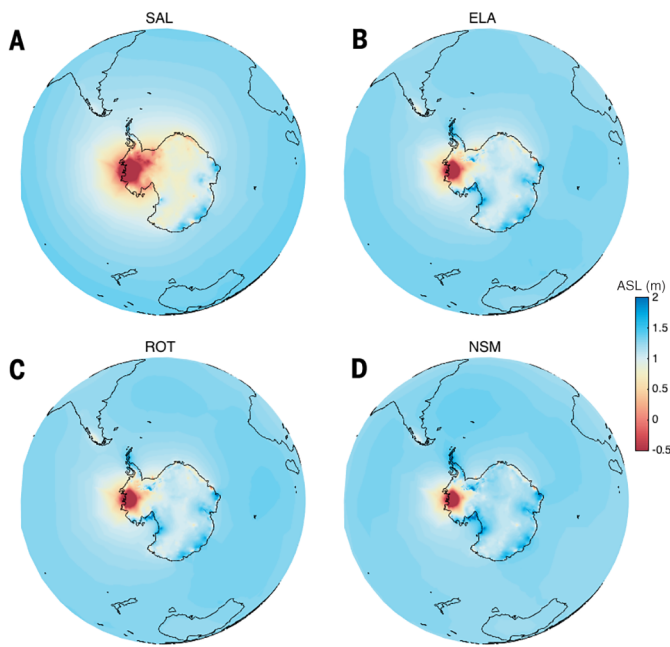


Fig. 3. ASL projection at model time 2350. The projection is determined for the UNC, EUS, SAL, ELA, ROT, and NSM models. All six models are described in Table 1. **(A to D)** Nonuniform ASL patterns for the models indicated. For the UNC model, ASL is constant at 1.3076 m, and for the EUS model, ASL is constant at 1.3160 m. Coastlines (40) are displayed in black. The other hemisphere is addressed in fig. S18. ASL in the continents should be interpreted as geoid height change plus the EUS value.

between the grounding line position of the UNC model versus the EUS model (Fig. 4, red versus yellow lines), with a positive feedback resulting in a EUS grounding-line position 1 to 2 km further upstream. With the SAL model, the feedback introduced is negative and of a much larger magnitude, with a differential in grounding-line position of 20 to 30 km (Fig. 4, red versus green lines). This is equivalent to 10% less migration in grounding line after 350 years. However, a larger negative feedback is introduced when taking into account elastic land uplift. This feedback delays grounding-line retreat significantly, resulting in a differential position in the grounding line of 100 to 120 km downstream of the UNC position (Fig. 4, red versus purple lines), which is equivalent to a 38% decrease in overall grounding-line migration after 350 years. As the next hierarchical level of complexity is included—ROT—only very minor additional effects are detected (Fig. 4, purple and blue lines, which are completely coincident), demonstrating that rotational feedback has a negligible impact on grounding-line retreat for Antarctica. Additional stabilization occurs (7, 8) through introduction of BGIA (Fig. 4, cyan versus purple lines) responsible for a small grounding-line differential (1 to 2 km), increasing to 10 km in some specific areas in the main trunk of TG (Fig. 4, inset).

Given that our BGIA time series are not interactively computed and are just a representation of past loading history, we carried out a second analysis in which we assessed the impact of three background models derived from a re-

cent GIA statistical study (26). The medium model corresponds to the average or expectancy rate. The lower- and higher-end models correspond to scenarios with the same probability as that of the average model that either minimize or maximize uplift in this region. For the TG area, the lower-end model sees BGIA signals around 0.6 mm/year, and the higher-end model sees BGIA signals around 2 mm/year. Results are displayed in fig. S3, showing a negligible impact of the lower-end BGIA models and a negative feedback of up to 20 km in specific areas from the higher-end model. This shows that stronger grounding-line stabilization could be expected from higher rates of GIA uplift, which is in line with the expectation of softer rheologies and larger background uplift rates in the area (1). Our results in terms of quantifying feedbacks in GLD (along the Fig. 4 gray flowline) and associated volume change (volume in sea-level equivalent) are summarized in Table 1. The relationship is not linear, with, for example, the NSM run (the run that encompasses all five processes above) exhibiting -38.5% grounding-line retreat versus the UNC run at 2350, translating into a -28.4% difference in volume change for TG. The traditional metric of volume above flotation used by modeling efforts—such as the Sea-level Response to Ice Sheet Evolution (SeaRISE) (32) or the Ice Sheet Modeling Inter-comparison Project 6 (ISMIP6) (33), and provided in Table 1 for reference—cannot be used to quantify sea-level equivalent because the assumption of a rigid surface bedrock is shown here to be in-

valid, with uplift tending to decrease volume above flotation.

The negative feedbacks from SAL and elastic uplift for WAIS are significant but not specific to the area. Because our model runs are global, the same analysis can be shown for the entire continent in fig. S4, showing negative feedbacks in areas of strong retreat, such as the tributary ice streams of the Ronne and Ross ice shelves (figs. S5 and S6). However, the impact in WAIS is particularly relevant because of the existing retrograde slope of the bedrock and the presence of a prominent bedrock trough upstream of TG, which triggers marine ice-sheet instability (23) and results in large ice thickness change rates upon ungrounding. In addition, strong ice-ocean interactions are captured for this area in our melt rate parameterization under the TG ice shelf (11). The melt rates computed for this area are much larger (reaching highest values of 60 to 80 m at the grounding line) than for other areas in Antarctica (34). The rate at which TG loses mass to the oceans starting year 2250 is strong enough as to generate changes in surface velocity of 3 km/year inland (figs. S11 and S12), resulting in dynamic changes in surface elevation of up to 45 m/year by 2500 (figs. S13 and S14). The changes in ice load are responsible for generating elastic uplift on the order of 3 to 5 cm/year by year 2100–2300, increasing to more than 20 cm/year at the onset of TG's dynamic retreat, culminating at 45 cm/year around year 2500 (figs. S15 and S16). This uplift rate generates large differences in the vertical position of the bedrock along TG flowlines (Fig. 4, flowline profile) on the order of tens of meters. The uplift rates have been independently validated (fig. S17) with a benchmark experiment (35).

When we monitored projected SLR generated by the retreat of TG and all glaciated areas around the world, a kink in the rise around year 2350 for four different cities was revealed (fig. S2). Before 2350, most of the SLR trend is due to the linearly extrapolated contribution of all glaciated areas around the world. The evolving contribution from TG after the time of the kink (the time at which the most dynamic retreat is initiated) is also delayed by elastic uplift. Shown in Fig. 5 is the corresponding change in ice volume (in meters-equivalent SLR) generated by the retreat of TG as relative mass change evolves in time from 0% in 2000 to 100% at 2500, when most of the collapse has occurred. The delay between UNC and NSM is 12% in terms of normalized mass change [corresponding to roughly 23 years at 2350 (fig. S1)]. This causes a negative feedback for the TG contribution to SLR of 0.12 m. This represents a 28.4% reduction in its SLR contribution. The differential in grounding-line migration evolves through time (figs. S7 and S9). By year 2300, the differential stands at ~ 50 to 80 km, and by year 2350, it has reached 100 to 120 km and holds above 80 km throughout year 2450. For corresponding TG ice volume change (Table 1), by year 2100 the negative feedback reaches -1.34% ; by year 2350, -28.4% ; and by year 2500, -9.9% . This implies that if we apply

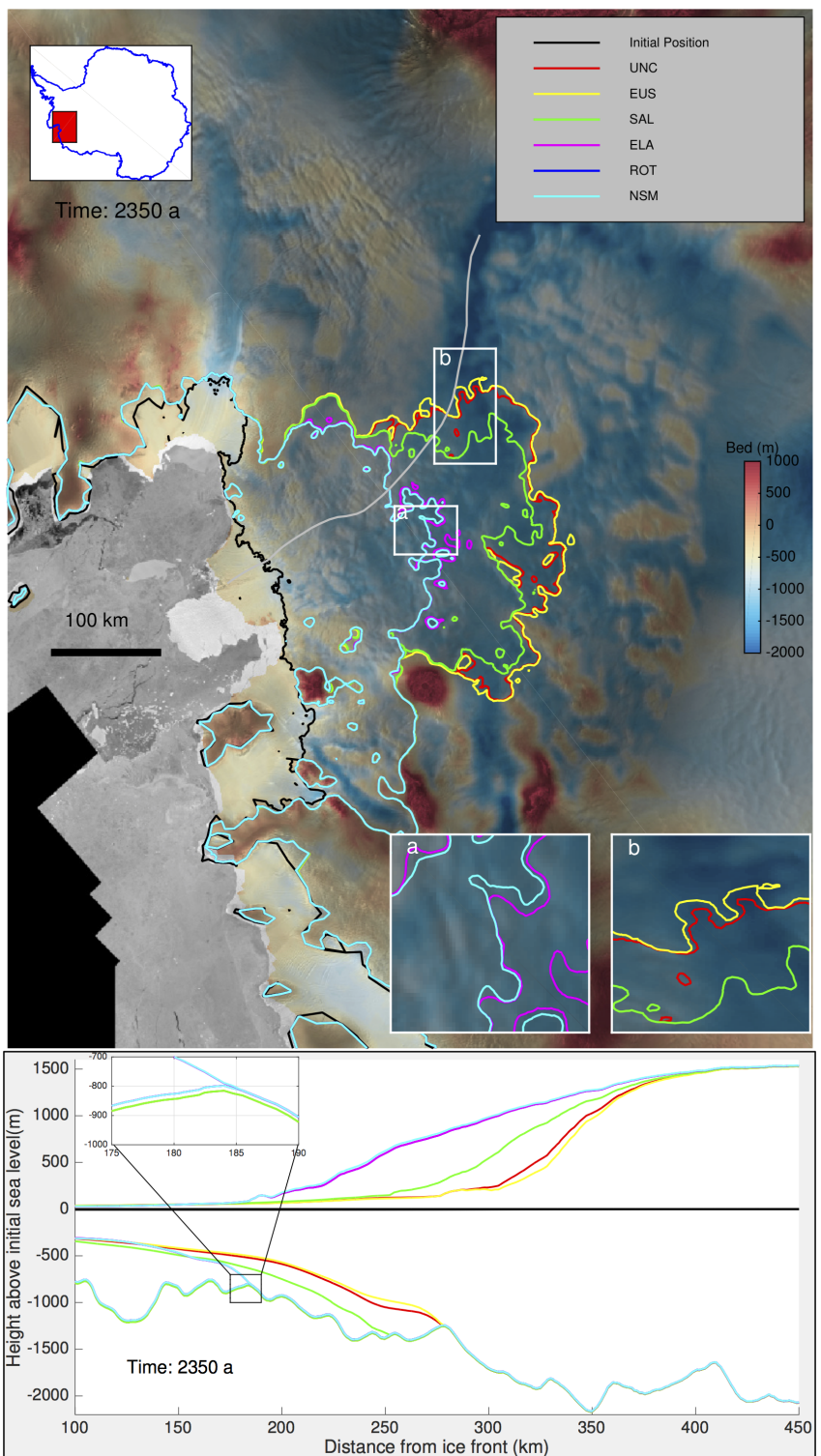


Fig. 4. Grounding-line projection for TG and PIG at model year 2350. (Top) The projection is carried out for the UNC, EUS, SAL, ELA, ROT, and NSM models. Initial grounding-line position at 2000 is displayed in black. Zooms on the grounding line in the deep interior of TG (a and b) are also displayed in the corresponding insets. Grounding-line positions are overlaid on a local bedrock topography map (supplementary materials, materials and methods). General location of the area in Antarctica is given in the top left inset. (Bottom) A section profile along the gray flowline at top is shown for the same six models, with surface, bedrock, and ice-shelf draft elevations plotted. (Inset) A zoom on the grounding line for the NSM, ROT, and ELA models, showing the uplifted versus initial bedrock at year 2350.

our sensitivity study to more realistic SLR projections that incorporate realistic climatologies, we would need to potentially take into account such dynamic effects in GLD and resulting sea-level contribution within two to three centuries. Projections toward 2100 CE should not be substantially affected by such negative feedback. In addition, a 1-km resolution is required, at least (figs. S7 and S8). Any coarsening past this resolution results in considerable delays in GLD, with a 1- to 8-km coarsened mesh for TG resulting in a delay of 160 years (fig. S8). Below 1-km resolution, our model is currently computationally too expensive. We therefore cannot infer whether convergence in uplift rates and grounding-line migration rates has been achieved. However, constraints in the bedrock topography are such that resolutions below 1 km have currently not been achieved by NASA's Operation IceBridge or any other measurement campaign. It would therefore be difficult to achieve realistic simulations below the 1-km threshold.

Discussion

For 21st-century projections (36, 37), the effects we have modeled are negligible. However, for the period starting 2250 and after, RSL projections that would not account for such dynamic geodetic effects run the risk of consistently overestimating (by 20 to 40%) RSL values (Table 1 and fig. S2B). Again, the impact of realistic climatologies in running such projections is difficult to assess, but we believe that our sensitivity study is robust enough to provide a better road map for making future projections. In general, our analysis suggests that any significant dynamic mass loss of an ice sheet, once triggered, cannot be realistically modeled if dynamic feedbacks (SAL, elastic uplift, and BGIA) are ignored. Inferences from current geodetic (uplift) measurements (1) that near-term stabilization is realized have to be treated with some caution. The main caveat is that the full high-resolution geometry of the outlet glacier and drainage basin must be considered. Our approach shows that significant stabilization in grounding-line migration occurs when uplift rates start approaching 10 cm/year for TG. In addition the offset between NSM (the most comprehensive run considered in our analysis) and UNC runs keeps increasing as time progresses after 2350 (fig. S2A). This means that the grounding-line migration differential is not compensated for as time passes by but rather keeps increasing between both models. This has strong implications for late Quaternary reconstructions of SLR, in which all the feedbacks associated with the NSM model need to be actively accounted for. For example, the inclusion of these solid-Earth processes will allow climate change modelers to improve their understanding of the time scales involved in reaching maximum coastal inundation levels during the extended warm periods of the late Quaternary that are now fairly well recorded in ocean sediment and ice core data sets (38).

The implications of a strong negative feedback, particularly from elastic uplift, are important

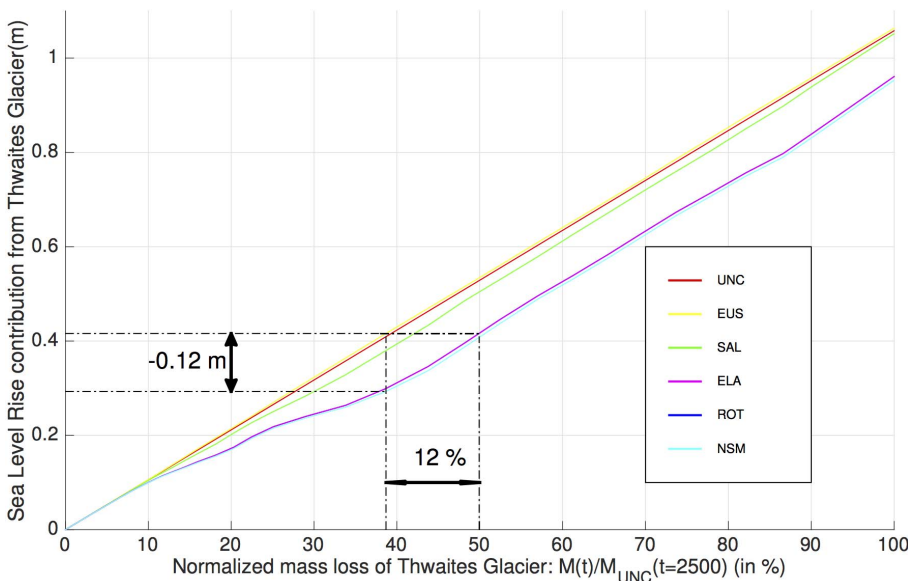


Fig. 5. 500-year contribution of TG to SLR (in meters SLR equivalent). The x axis represents the normalized mass loss (in percent) defined here as the ratio of mass loss $M(t)$ from TG at time t to final mass loss $M_{UNC}(t = 2500)$ of TG for the UNC control run at time $t = 2500$. This results in a UNC SLR contribution that scales linearly with normalized mass loss. This linearity breaks down for the other runs. Normalized mass loss of the UNC run is acting here as our absolute time reference. A plot with the corresponding timeline (in years) is provided in fig. S1. Approximately 0.42 m SLR is achieved for 38% of TG normalized mass loss in the UNC run, whereas including all solid-Earth processes, the same amount of SLR is achieved only after an additional 12% mass loss occurs [or after a 23-year delay (fig. S1)], which corresponds to an offset of 0.12 m in SLR.

in that it will lead to a revision of current SLR projections past 2250. Our results over the whole Antarctic show that this feedback manifests mainly for the WAIS area, where ice-ocean interactions and marine ice sheet instability combine to generate substantial uplift. There is an increasing body of evidence suggesting that the upper mantle under WAIS is softer than the rest of Antarctica (21, 39), which has not been considered here. This means that AIS could experience GLD negative feedbacks even stronger than 38.5% and delays in the corresponding SLR spike of more than half a century. Preliminary estimates from (21) suggest that a doubling of the elastic contribution should be considered as an estimate for the total viscoelastic feedback experienced by WAIS glaciers on time scales of 300 years. This also means that current models systematically overestimate SLR projections past 2250 and that the timing of paleo reconstructions currently used to validate and constrain such projections (36) might be substantially affected.

REFERENCES AND NOTES

- V. R. Barletta et al., Observed rapid bedrock uplift in Amundsen Sea Embayment promotes ice-sheet stability. *Science* **360**, 1335–1339 (2018). doi: [10.1126/science.aao1447](https://doi.org/10.1126/science.aao1447); pmid: [29930133](#)
- J. Kingslake et al., Extensive retreat and re-advance of the West Antarctic Ice Sheet during the Holocene. *Nature* **558**, 430–434 (2018). doi: [10.1038/s41586-018-0208-x](https://doi.org/10.1038/s41586-018-0208-x); pmid: [29899456](#)
- W. E. Farrell, J. A. Clark, On postglacial sea level. *Geophys. J. Int.* **46**, 647–667 (1976). doi: [10.1111/j.1365-246X.1976.tb01252.x](https://doi.org/10.1111/j.1365-246X.1976.tb01252.x)
- K. Lambeck, *The Earth's Variable Rotation, Geophysical Causes and Consequences* (Cambridge Univ. Press, 2009).
- W. R. Peltier, The impulse response of a Maxwell Earth. *Rev. Geophys.* **12**, 649 (1974). doi: [10.1029/RG012i004p00649](https://doi.org/10.1029/RG012i004p00649)
- N. Gomez, J. X. Mitrovica, M. E. Tamisiea, P. U. Clark, A new projection of sea level change in response to collapse of marine sectors of the Antarctic Ice Sheet. *Geophys. J. Int.* **180**, 623–634 (2010). doi: [10.1111/j.1365-246X.2009.04419.x](https://doi.org/10.1111/j.1365-246X.2009.04419.x)
- N. Gomez, J. X. Mitrovica, P. Huybers, P. U. Clark, Sea level as a stabilizing factor for marine-ice-sheet grounding lines. *Nat. Geosci.* **3**, 850–853 (2010). doi: [10.1038/ngeo1012](https://doi.org/10.1038/ngeo1012)
- S. Adhikari et al., Future Antarctic bed topography and its implications for ice sheet dynamics. *Solid Earth* **5**, 569–584 (2014). doi: [10.5194/se-5-569-2014](https://doi.org/10.5194/se-5-569-2014)
- H. Konrad, I. Sasgen, D. Pollard, V. Klemann, Potential of the solid-Earth response for limiting long-term West Antarctic Ice Sheet retreat in a warming climate. *Earth Planet. Sci. Lett.* **432**, 254–264 (2015). doi: [10.1016/j.epsl.2015.10.008](https://doi.org/10.1016/j.epsl.2015.10.008)
- E. Rignot, J. Mouginot, M. Morlighem, H. Seroussi, B. Scheuchl, Widespread, rapid grounding line retreat of Pine Island, Thwaites, Smith, and Kohler glaciers, West Antarctica, from 1992 to 2011. *Geophys. Res. Lett.* **41**, 3502–3509 (2014). doi: [10.1002/2014GL060140](https://doi.org/10.1002/2014GL060140)
- H. Seroussi et al., Continued retreat of Thwaites Glacier, West Antarctica, controlled by bed topography and ocean circulation. *Geophys. Res. Lett.* **44**, 6191–6199 (2017). doi: [10.1002/2017GL072910](https://doi.org/10.1002/2017GL072910)
- E. Rignot, J. Mouginot, B. Scheuchl, Ice flow of the Antarctic ice sheet. *Science* **333**, 1427–1430 (2011). doi: [10.1126/science.1208336](https://doi.org/10.1126/science.1208336); pmid: [21852457](#)
- L. Favier et al., Retreat of Pine Island Glacier controlled by marine ice-sheet instability. *Nat. Clim. Chang.* **4**, 117–121 (2014). doi: [10.1038/nclimate2094](https://doi.org/10.1038/nclimate2094)
- K. Matsuoka et al., Antarctic ice rises and ripples: Their properties and significance for ice-sheet dynamics and evolution. *Earth Sci. Rev.* **150**, 724–745 (2015). doi: [10.1016/j.earscirev.2015.09.004](https://doi.org/10.1016/j.earscirev.2015.09.004)
- G. H. Gudmundsson, J. Krug, G. Durand, L. Favier, O. Gagliardini, The stability of grounding lines on retrograde slopes. *Cryosphere* **6**, 1497–1505 (2012). doi: [10.5194/tc-6-1497-2012](https://doi.org/10.5194/tc-6-1497-2012)
- S. Anandakrishnan, D. D. Blankenship, R. B. Alley, P. L. Stoffa, Influence of subglacial geology on the position of a West Antarctic ice stream from seismic observations. *Nature* **394**, 62–65 (1998). doi: [10.1038/27889](https://doi.org/10.1038/27889)
- E. J. Rignot, Fast recession of a West Antarctic glacier. *Science* **281**, 549–551 (1998). doi: [10.1126/science.281.5376.549](https://doi.org/10.1126/science.281.5376.549); pmid: [9677195](#)
- I. Joughin, B. E. Smith, B. Medley, Marine ice sheet collapse potentially under way for the Thwaites Glacier Basin, West Antarctica. *Science* **344**, 735–738 (2014). doi: [10.1126/science.1249055](https://doi.org/10.1126/science.1249055); pmid: [24821948](#)
- F. Pattyn et al., Grounding-line migration in plan-view marine ice-sheet models: Results of the ice2sea MISMIP3d intercomparison. *J. Glaciol.* **59**, 410–422 (2013). doi: [10.3189/2013JoG12J129](https://doi.org/10.3189/2013JoG12J129)
- B. de Boer, P. Stocchi, P. L. Whitehouse, R. S. W. van de Wal, Current state and future perspectives on coupled ice-sheet – sea-level modelling. *Quat. Sci. Rev.* **169**, 13–28 (2017). doi: [10.1016/j.quascirev.2017.05.013](https://doi.org/10.1016/j.quascirev.2017.05.013)
- C. C. Hay et al., Sea level fingerprints in a region of complex Earth structure: The case of WAIS. *J. Clim.* **30**, 1881–1892 (2017). doi: [10.1175/JCLI-D-16-0388.1](https://doi.org/10.1175/JCLI-D-16-0388.1)
- R. Bindschadler et al., Ice-sheet model sensitivities to environmental forcing and their use in projecting future sea level (the SeaRISE project). *J. Glaciol.* **59**, 195–224 (2013). doi: [10.3189/2013JoG12J125](https://doi.org/10.3189/2013JoG12J125)
- J. Weertman, Stability of the junction of an ice sheet and an ice shelf. *J. Glaciol.* **13**, 3 (1974). doi: [10.1017/S0022143000023327](https://doi.org/10.1017/S0022143000023327)
- G. A. Milne, J. X. Mitrovica, Postglacial sea-level change on a rotating Earth. *Geophys. J. Int.* **133**, 1–19 (1998). doi: [10.1046/j.1365-246X.1998.1331455.x](https://doi.org/10.1046/j.1365-246X.1998.1331455.x)
- E. Larour, E. R. Ivins, S. Adhikari, Should coastal planners have concern over where land ice is melting? *Sci. Adv.* **3**, e1700537 (2017). doi: [10.1126/sciadv.1700537](https://doi.org/10.1126/sciadv.1700537); pmid: [29152565](#)
- L. Caron et al., GIA model statistics for GRACE hydrology, cryosphere, and ocean science. *Geophys. Res. Lett.* **45**, 2203–2212 (2018). doi: [10.1002/2017GL076644](https://doi.org/10.1002/2017GL076644)
- E. Larour, H. Seroussi, M. Morlighem, E. Rignot, Continental scale, high order, high spatial resolution, ice sheet modeling using the Ice Sheet System Model (ISSM). *J. Geophys. Res.* **117**, F01022 (2012).
- S. Adhikari, E. R. Ivins, E. Larour, ISSM-SESAW v1.0: Mesh-based computation of gravitationally consistent sea-level and geodetic signatures caused by cryosphere and climate driven mass change. *Geosci. Model Dev.* **9**, 1087–1109 (2016). doi: [10.5194/gmd-9-1087-2016](https://doi.org/10.5194/gmd-9-1087-2016)
- S. Adhikari, E. R. Ivins, Climate-driven polar motion: 2003–2015. *Sci. Adv.* **2**, e1501693 (2016). doi: [10.1126/sciadv.1501693](https://doi.org/10.1126/sciadv.1501693); pmid: [27152348](#)
- J. L. Bamber, R. E. M. Riva, B. L. A. Vermeersen, A. M. LeBrocq, Reassessment of the potential sea-level rise from a collapse of the West Antarctic Ice Sheet. *Science* **324**, 901–903 (2009). doi: [10.1126/science.1169335](https://doi.org/10.1126/science.1169335); pmid: [19443778](#)
- J. X. Mitrovica, N. Gomez, P. U. Clark, The sea-level fingerprint of West Antarctic collapse. *Science* **323**, 753 (2009). doi: [10.1126/science.1166510](https://doi.org/10.1126/science.1166510); pmid: [19197056](#)
- S. Nowicki et al., Insights into spatial sensitivities of ice mass response to environmental change from the SeaRISE ice sheet modeling project I: Antarctica. *J. Geophys. Res.* **118**, 1002–1024 (2013).
- S. M. J. Nowicki et al., Ice Sheet Model Intercomparison Project (ISMIP6) contribution to CMIP6. *Geosci. Model Dev.* **9**, 4521–4545 (2016). doi: [10.5194/gmd-9-4521-2016](https://doi.org/10.5194/gmd-9-4521-2016); pmid: [29697697](#)
- M. P. Schodlok, D. Menemenlis, E. J. Rignot, Ice shelf basal melt rates around Antarctica from simulations and observations. *J. Geophys. Res. Oceans* **121**, 1085–1109 (2016). doi: [10.1002/2015JC011117](https://doi.org/10.1002/2015JC011117)
- G. Spada et al., A benchmark study for glacial isostatic adjustment codes. *Geophys. J. Int.* **185**, 106–132 (2011). doi: [10.1111/j.1365-246X.2011.04952.x](https://doi.org/10.1111/j.1365-246X.2011.04952.x)
- R. M. DeConto, D. Pollard, Contribution of Antarctica to past and future sea-level rise. *Nature* **531**, 591–597 (2016). doi: [10.1038/nature17145](https://doi.org/10.1038/nature17145); pmid: [27029274](#)
- C. Ritz et al., Potential sea-level rise from Antarctic ice-sheet instability constrained by observations. *Nature* **528**, 115–118 (2015). pmid: [26580020](#)
- Past Interglacials Working Group of PAGES, Interglacials of the last 800,000 years. *Rev. Geophys.* **54**, 162–219 (2016). doi: [10.1002/2015RG000482](https://doi.org/10.1002/2015RG000482)
- W. van der Wal, P. L. Whitehouse, E. J. Schrama, Effect of GIA models with 3D composite mantle viscosity on GRACE mass balance estimates for Antarctica. *Earth Planet. Sci. Lett.* **414**, 134–143 (2015). doi: [10.1016/j.epsl.2015.01.001](https://doi.org/10.1016/j.epsl.2015.01.001)

40. P. Wessel, W. H. F. Smith, A global, self-consistent, hierarchical, high-resolution shoreline database. *J. Geophys. Res. Oceans* **101** (B4), 8741–8743 (1996). doi: [10.1029/96JB00104](https://doi.org/10.1029/96JB00104)

ACKNOWLEDGMENTS

The research was carried out at the Jet Propulsion Laboratory (JPL), California Institute of Technology, under a contract with the National Aeronautics and Space Administration (NASA). Resources supporting this work were provided by the NASA High-End Computing (HEC) Program through the NASA Advanced Supercomputing (NAS) Division at Ames Research Center. During the time elapsed between electronic and printed versions, G. Milne read the manuscript and found two serious typographical errors, and we are indebted to him for communicating these to us promptly. **Funding:** This work was funded by JPL Research,

Technology and Development Program grant #01STCR R.17.235.118 (S.A.). It was also funded by the following programs at NASA: Cryospheric sciences under grants 105393 509496.02.08.08.53 and 105393 444491.02.04.01.80 (E.L. and N.S.) and grant 105393 281945.02.53.04.07 (H.S.), Modeling Analysis and Prediction under grants 105479 509496.02.08.10.07 (E.L. and N.S.) and 105479 509496.02.08.08.49 (H.S.), GRACE Science Team under grant E.8.11 (E.L.), Sea-Level Science Team under grants 105393 509496.02.08.10.65 (E.L., E.I., L.C., N.S., and S.A.) and 105393 281945.02.53.03.97 (E.I.), and Earth System and Interior under grant 105526-281945.02.47.03.86. It was also funded by NFS grant 1739031 (M.M.). **Author contributions:** E.L., S.A., E.I., L.C., and H.S. contributed to the theory. E.L. led the calculations. E.I., L.C., and S.A. assisted with interpretation of the results. M.M. assisted with modeling of the bedrock. H.S. assisted with modeling of ice/ocean interactions. N.S. assisted with model setup. All authors contributed

to the writing of the paper. **Competing interests:** The authors declare that they have no competing interests. **Data and materials availability:** All data are available in the manuscript or the supplementary materials. All simulations were carried out using the Ice Sheet System Model, which is freely and publicly available at <http://issm.jpl.nasa.gov>.

SUPPLEMENTARY MATERIALS

science.sciencemag.org/content/364/6444/eaav7908/suppl/DC1

Materials and Methods

Figs. S1 to S19

References (41–47)

22 October 2018; accepted 12 April 2019

Published online 25 April 2019

10.1126/science.aav7908

Slowdown in Antarctic mass loss from solid Earth and sea-level feedbacks

E. Larour, H. Seroussi, S. Adhikari, E. Ivins, L. Caron, M. Morlighem and N. Schlegel

Science 364 (6444), eaav7908.
DOI: 10.1126/science.aav7908 originally published online April 25, 2019

An uplifting effect

The rise in sea level that is occurring from the melting of Antarctica is only going to accelerate as climate warms. However, Larour *et al.* report that crustal uplift in the Amundsen Sea sector is helping to reduce grounding line retreat, thereby stabilizing the ice sheet and slowing its rate of mass loss (see the Perspective by Steig). This effect will not stop or reverse ice sheet loss, but it could delay the progress of dynamic mass loss of Thwaites Glacier by approximately 20 years.

Science, this issue p. eaav7908; see also p. 936

ARTICLE TOOLS

<http://science.scienmag.org/content/364/6444/eaav7908>

SUPPLEMENTARY MATERIALS

<http://science.scienmag.org/content/suppl/2019/04/24/science.aav7908.DC1>

RELATED CONTENT

<http://science.scienmag.org/content/sci/364/6444/936.full>

REFERENCES

This article cites 46 articles, 8 of which you can access for free
<http://science.scienmag.org/content/364/6444/eaav7908#BIBL>

PERMISSIONS

<http://www.scienmag.org/help/reprints-and-permissions>

Use of this article is subject to the [Terms of Service](#)

Science (print ISSN 0036-8075; online ISSN 1095-9203) is published by the American Association for the Advancement of Science, 1200 New York Avenue NW, Washington, DC 20005. The title *Science* is a registered trademark of AAAS.

Copyright © 2019 The Authors, some rights reserved; exclusive licensee American Association for the Advancement of Science. No claim to original U.S. Government Works